Anisotropic Dark Stars in Rastall Modified Gravity: Energy Conditions, Tidal Deformability and Moment of Inertia

Jessie Chandra[1], Anto Sulaksono[1]
Departemen Fisika, FMIPA, Universitas Indonesia, Depok, Indonesia.
jessie11@alumni.ui.ac.id
anto.sulaksono@sci.ui.ac.id
(Submitted on 10.11.2025; Accepted on 19.01.2026)

Abstract. We construct anisotropic dark stars using the generalized Chaplygin gas (GCG) equation of state, where the GCG is an exotic fluid model that unifies dark matter and dark energy. This approach allows for an elegant theoretical treatment of dark stars. We apply the quasi-local anisotropy model of Horvat et al., which introduces direction-dependent pressures at each point inside the star, and test the strong and dominant energy conditions, which serve as criteria for ensuring physically plausible behavior in the stellar interior. Our study extends to Rastall gravity, a modified theory of gravity in which the usual conservation of energy and momentum is relaxed. By solving the modified Tolman - Oppenheimer - Volkoff equations, which describe the equilibrium structure of spherically symmetric stars, we determine the macroscopic properties of GCG dark stars. Our results demonstrate that the Rastall parameter, which characterizes the deviation from standard energy conservation, has a significant impact on the mass - radius relations, compactness, and tidal effects, while anisotropy further modifies equilibrium properties. Energy condition tests confirm that only specific ranges of the Rastall and anisotropy parameter values allow for physical viability.
Key words: dark matter, dark energy stars, modified gravity, tidal deformability, moment of inertia, anisotropy

1 Introduction

General Relativity (GR) was formulated by Albert Einstein in 1915. It remains the standard framework for describing gravity as the curvature of spacetime produced by mass and energy. This framework explains the dynamics of massive astrophysical objects and the universe's large-scale structure [Glendenning, 2007]. However, several fundamental problems, including the nature of dark matter and dark energy, remain unresolved within pure GR.

Rastall modified gravity is a well-studied alternative to GR [Rastall, 1972]. It relaxes the requirement that energy and momentum must always remain constant in curved spacetime. In this theory, changes in energy and momentum are directly tied to a property of spacetime geometry known as the Ricci scalar. This approach offers a broader perspective, allowing energy and momentum variations to help explain unresolved astrophysical phenomena, such as dark matter and dark energy [Rastall, 1972]. Recent studies have examined compact stars and exotic matter within Rastall's framework. These studies suggest that such changes can influence our observations of stars.

Although it has been argued that Rastall gravity is formally equivalent to Einstein gravity with a mere rearrangement of the energy - momentum tensor [Visser, 2018], this interpretation has been critically examined in other studies. Darabi et al. compared the two gravity theories and demonstrated that such a redefinition modifies the physical content of Rastall gravity [Darabi et al., 2018]. Unlike Einstein gravity, Rastall gravity is fundamentally characterized by a non-minimal coupling between matter and geometry and by modified conservation laws. We can regard Rastall gravity as a specific case of the

broader class of $f(R,T)$ gravity [Fisher and Carlson, 2019,Shabani et al., 2022, Harko and Moraes, 2020], further emphasizing its departure from standard GR. Chagoya et al. [Chagoya et al., 2023] conducted a study on the equivalence of parameterized fluids in Rastall gravity and GR, which showed that the same matter translates to different effective matter properties when switching between the two gravity frameworks (e.g. cold dark matter fluid in Rastall gravity corresponds to warm dark matter in GR). Rastall gravity has also been applied to numerous astrophysical systems and in cosmology [Sakti et al., 2020, Abbas and Shahzad, 2018, Abbas and Shahzad, 2019, Moradpour et al., 2017b,Prihadi et al., 2020,Sakti et al., 2022,Sakti and Sulaksono, 2021,Oliveira et al., 2015].

The non-conserved energy-momentum tensor in Rastall gravity is particularly appealing for the dark matter (DM) and dark energy (DE) studies. The lack of observational evidence of DM and DE allows the possibility of a framework with violations of the usual GR conservation laws. Such non-conserved situations have also been supported by phenomenological indications from relativistic diffusion models [Calogero and Velten, 2013] and cosmological particle creation processes [Moradpour et al., 2017a]. In this framework, the divergence of the energy-momentum tensor is proportional to the Ricci scalar, where the conservation law is obeyed in the case of a flat geometry.

Fundamental principles in physics are usually derived from action principles, which is an aspect missing in Rastall gravity. Although this can be a weakness of Rastall gravity, it has been investigated in several works how a Lagrangian construction may be possible in the Rastall framework. One study constructed a Lagrangian using non-minimal couplings between matter and geometry and showed that it reproduced Rastall's field equations, while also leading to consistent physical results (i.e. Gödel-type solutions) [Moraes and Santos, 2019]. In another study, a Lagrangian was constructed using a variational principle and the Rastall field equations were derived from it [dos Santos and Nogales, 2017]. Their method was applied to cosmological models, which were successfully compared with observational data. Fabris et al. also analyzed the possibility of a Lagrangian formulation for specific cases of the Rastall framework through studying the similarities between Rastall gravity and two $f(R)$ gravity theories: $f(R,L_m)$ and $f(R,T)$ [Fabris et al., 2023]. These two $f(R)$ theories also violate the conservation of the energy-momentum tensor while still preserving diffeomorphism invariance.

In our work, we have chosen to apply Rastall gravity due to its simple and minimal modification. Modifying only the energy–momentum tensor, without introducing new fields or higher-order curvature terms, makes the theory mathematically tractable while still allowing for new physical effects.

Recently, research within the Rastall framework has increased notably. This includes studies analyzing gravitational-wave data and examining how static neutron stars deform in a weak external tidal field. In these scenarios, tidal Love numbers are smaller in Rastall gravity than in GR [Meng and Liu, 2021]. The Rastall framework has also been applied to study quark matter; for instance, quark stars have been examined with an interacting quark matter equation of state (EoS) in Rastall gravity, revealing effects on stellar mass-radius relations and the adiabatic index [Banerjee et al., 2024], and compara-

tive studies of magnetized quark star deformations under Einstein and Rastall gravity have previously been conducted [Rizaldy and Sulaksono, 2019].

There have also been studies explaining the stability of compact stars in Rastall gravity, showing that the stability conditions depend mainly on the Rastall parameter [Pretel and Mota, 2024], as well as studies of anisotropic stars using the Krori and Barua metric, which confirm that higher Rastall parameters yield larger maximum masses while still agreeing with observations [Biswas et al., 2025]. Rastall gravity is also applied beyond compact stars. For instance, black holes and exotic objects have been explored in Rastall gravity using Kerr/CFT correspondence [Sakti et al., 2022]. They demonstrated that the Rastall coupling alters the entropy, absorption cross-sections, and echo time delays, which can be observed as potential signatures of the theory.

Dark matter is believed to constitute about 27 percent of the universe's mass-energy content and it remains a major unresolved issue in modern astrophysics. Its existence is inferred from galactic rotation curves, gravitational lensing, cosmic microwave background (CMB) anisotropies, and the formation of large-scale structure. However, DM has not been directly detected. Proposed candidates and models include the Lambda Cold Dark Matter (ΛCDM) paradigm [Weinberg et al., 2012], Weakly Interacting Massive Particles (WIMPs) [Gelmini, 2017], and axions [Chadha-Day et al., 2022]. Unified dark fluid models such as the Chaplygin gas (GCG) [Kamenshchik et al., 2001] have also been proposed. Additional dark energy models include those represented by a phantom field [Sakti and Sulaksono, 2021].

The concept of a dark star, a compact astrophysical object composed predominantly of dark matter and/or dark energy, extends these considerations to the field of stellar astrophysics. The GCG equation of state (EoS) has been widely adopted as a unified description of DM and DE within a single fluid. This model is consistent with observational tests involving gravitational lensing, the CMB, and gamma-ray bursts, while maintaining a mathematically simple EoS [Bento et al., 2002]. In this research, we assume a stellar configuration entirely composed of the simplified modified Chaplygin gas (SMCG). Other versions of the Chaplygin gas have also been studied as possible equations of state for the dark stars (see Sec. 2). However, the SMCG model is particularly appealing due to its mathematical simplicity. While it is more realistic for compact objects to be composed of multiple components (i.e. a mixture of ordinary matter, dark matter, and dark energy), such fluid system may introduce extra free parameters, making it more difficult to focus on the specific effects of the gravitational framework. To date, observational evidence regarding the composition of dark stars is still lacking. Because of this uncertainty, we find it reasonable to employ an idealized, simple model like the SMCG at present.

Since our constructed dark stars have not been officially confirmed by observations, they remain a theoretical prediction. However, recent developments indicate that this situation may change in the near future. Several observations from the James Webb Space Telescope have revealed massive objects with high luminosities, which have been proposed as potential dark star candidates [Ilie et al., 2023, Ilie et al., 2025]. Although these findings and their propositions are still under debate, they demonstrate that observational tests of dark star models are becoming increasingly feasible. Accordingly, we conduct this re-

search with the aim of developing a possible theoretical framework that can be confirmed or refuted once reliable observational data are acquired.

An additional layer of complexity arises from anisotropy in compact stars, where radial and tangential pressures differ. Such anisotropies can result from various physical mechanisms and may be essential for describing exotic states of matter, including dark sector candidates [Cadoni et al., 2020]. Several pressure anisotropy prescriptions are used, such as the Bowers-Liang model [Bowers and Liang, 1974] and the quasi-local model proposed by Horvat et al. [Horvat et al., 2011].

In 2023, Pretel constructed dark stars using a simplified version of the GCG model within the GR framework and analyzed their properties by introducing an anisotropy factor from the quasi-local model of Horvat et al. The study examined the dimensionless tidal deformability and the moment of inertia, focusing on anisotropic Chaplygin dark stars in hydrostatic equilibrium [Pretel, 2023].

This work investigates the behavior of anisotropic dark stars described by the GCG equation of state within the Rastall framework. Previous studies have not systematically examined the energy conditions (ECs) in this context. ECs are crucial for evaluating the physical plausibility of stellar configurations and ensuring their structural viability. In modified gravity theories with a non-conserved energy–momentum tensor, structures may violate physical conditions if parameters exceed certain limits. The introduction of anisotropic perturbations to the EoS can result in extreme pressure variations, potentially leading to cracking phenomena. This study explicitly tests the dominant and strong ECs to ensure that the resulting stellar models remain physically viable. Such scrutiny is necessary to confirm that the configurations represent realistic anisotropic dark stars rather than mathematical artifacts of the modified theory.

This paper is organized as follows: In Sec. 2, we introduce our dark star EoS (the GCG equation). In Sec. 3, we introduce the quasi-local anisotropy model to constrain pressure distributions. In Sec. 4, we present the Rastall modified gravity field equations, as well as the modified TOV equations. Sec. 5 discusses the tidal deformability of the star, while Sec. 6 discusses the moment of inertia and rotational equations. In Sec. 7, physical constraints and energy conditions are laid out. We discuss our results in Sec. 8. Finally, conclusions are summarized in Sec. 9.

2 Equation of State

In this section, we briefly discuss the EoS that describes matter in dark stars. Multiple observations have shown that the universe is expanding with an acceleration caused by negative pressure from DM and DE. Within this context, the Chaplygin gas was introduced in 2001, within the framework of FRW cosmology, as a model of a perfect exotic fluid [Kamenshchik et al., 2001]. This model is considered to be the "pure Chaplygin gas." In 2002, a modified Chaplygin gas (MCG) was introduced and developed [Bento et al., 2002, Benaoum, 2002], where new parameters were added. Alongside these, alternative EoSs for dark stars have also been proposed in the literature, including phantom and quintessence scalar field models, phenomenological extensions with power-law

and logarithmic corrections to pressure, as well as anisotropic fluid descriptions motivated by nuclear and QCD effects [Smerechynskyi et al., 2021, Bhar, 2021, Yazadjiev, 2011].

Despite these options, all the aforementioned models depict stars predominantly composed of DE. Notably, the Chaplygin gas family of models remains particularly appealing because it provides a unified description of DM and DE, supporting the possibility of DM and DE being different manifestations of the same substance [Xu et al., 2012, Bento et al., 2002]. Further strengthening its relevance, the Chaplygin gas model is consistent with various cosmological datasets (e.g., the gravitational-wave signal GW190814 interpreted as a compact star [Abbott et al., 2020]), and offers a mathematically tractable form suitable for stellar structure analyses. For these reasons, we adopt the Chaplygin-type EoS as the framework for our work.

The MCG model can be described by the equation of state:

$$p_{(\mathrm{MCG})} = A\epsilon - \frac{B}{\epsilon^C}. \tag{1}$$

To restrict the construction of fluids with infinite mass, the exponential constant is physically acceptable in the range $0 \leq C \leq 1$. In this research, a simplified version of the MCG model (SMCG), where $C = 1$, will be used. The SMCG model has been studied and verified in several past studies [Pretel, 2023, Panotopoulos et al., 2021, Rahaman et al., 2010, Bhar et al., 2018, Tello-Ortiz et al., 2020, Estevez-Delgado et al., 2021]. Building on this simplification, several works, including analyses of Planck 2015 CMB anisotropy data, have shown that the case where $C = 1$ is a sufficiently good fit to existing observations, hence there is no need to add more degrees of freedom. In the following, we use the simplified MCG equation of state in Eq. (1) with $C = 1$ while simultaneously testing a range of values for the anisotropy model in Sec. 3. We will also use the numerical values of the constants A and B that correspond to one of the anisotropic dark star models favored by observational pulsar measurements, as used by Pretel [Pretel, 2023].

- $A = 0.3$ [dimensionless],
- $B = 6.0\mu$, where $\mu = 10^{-20}$ m^{-4}.

These parameters allow the construction of a compact object with a maximum mass slightly smaller than the neutron star pulsars J1614-2230 [Demorest et al., 2010] and J0348+0432 [Antoniadis et al., 2013]. This assumes an isotropic condition for the dark star. In this research, we consider these parameters to be suitable. We consider the possibility of extending the maximum mass upward once our Chaplygin dark star is subjected to anisotropic effects, particularly under modifications from Rastall gravity. This leaves room for configurations that may reach the observational data limits that might be provided in the future. A brief discussion of anisotropic effects and Rastall gravity will be given in the next section.

3 Quasi-local Anisotropy Model

Dark stars are a class of exotic stars in which the pressure of matter may become anisotropic. Therefore, in this work, we adopt this assumption. Several studies have also explored the possibility of constructing dark matter as

an anisotropic fluid [Pretel, 2023]. In compact stars, a state of anisotropy means that the pressure inside the star does not always equal its radial pressure (radial pressure $\neq$ tangential pressure). Anisotropic matter can lead to inhomogeneities, which could be responsible for the formation of DM and DE [Cadoni et al., 2020]. Over the years, numerous anisotropy models have been proposed. Some popular models include the Bowers-Liang model [Bowers and Liang, 1974] and the quasi-local model proposed by Horvat et al. [Horvat et al., 2011]. Many of these approaches rely on a phenomenological ansatz that introduces a functional relation between the radial and tangential pressures without being directly connected to a fundamental physical mechanism. While such models are useful for exploring the qualitative role of anisotropy, we adopt the anisotropy model proposed by Horvat et al., particularly because it exhibits a quasi-local dependence of the anisotropy on the compactness of the star. This framework has the advantage of being more physically grounded and dynamically consistent than many other anisotropy models. With the natural unit system ($c = G = 1$), the anisotropic matter is expressed through the variable σ:

$$\sigma = \alpha \left(\frac{2m}{r} \right) p_r, \tag{2}$$

where α is a dimensionless parameter that determines the anisotropy factor σ, which is defined as

$$\sigma = p_t - p_r. \tag{3}$$

In this work, we study the allowed values of α by testing the energy conditions for compact objects.

4 Rastall Modified Gravity

A fundamental equation in the theory of GR is the Einstein field equation (EFE):

$$R_{\mu\nu} - \frac{1}{2} g_{\mu\nu} R + \Lambda g_{\mu\nu} = \frac{8\pi G}{c^4} T_{\mu\nu}, \tag{4}$$

where $R_{\mu\nu}$ is the Ricci curvature tensor, $g_{\mu\nu}$ is the metric tensor, R is the Ricci scalar, Λ is the cosmological constant, G is the gravitational constant, c is the speed of light in vacuum, and $T_{\mu\nu}$ is the stress-energy tensor (stress-energy-momentum tensor). For the stars, Λ plays no role, and the EFE reduces to:

$$G_{\mu\nu} = R_{\mu\nu} - \frac{1}{2} g_{\mu\nu} R = 8\pi T_{\mu\nu}. \tag{5}$$

Unlike standard GR, Rastall gravity introduces a non-conserved stress-energy tensor and a nonminimal coupling between matter and geometry. This approach enables greater flexibility in modeling dense stars, including the incorporation of anisotropic matter.

Building on these distinctions, the gravity proposed by Rastall is not drastically different from the standard Einstein gravity. Rastall modified gravity

introduced a new free parameter γ, which replaces the factor 1 in the Ricci scalar term of EFE. The modified EFE is as follows:

$$R_{\mu\nu} - \frac{\gamma}{2} g_{\mu\nu} R = 8\pi T_{\mu\nu}. \tag{6}$$

For an unperturbed, static, spherically symmetric compact star, a suitable metric can be written as:

$$ds^2 = -e^{2\nu(r)} dt^2 + e^{2\lambda(r)} dr^2 + r^2(d\theta^2 + \sin^2\theta\, d\phi^2). \tag{7}$$

The Rastall field equation in Eq. (6) can be rewritten by setting the left-hand side equal to Einstein's field equation and the right-hand side $T_{\mu\nu}$ plus correction term. This result can be considered as GR with a modification of the matter or with effective matter.

$$G_{\mu\nu} = R_{\mu\nu} - \frac{1}{2} g_{\mu\nu} R = 8\pi (T_{\mu\nu} - \beta T g_{\mu\nu}). \tag{8}$$

T is the trace of $T_{\mu\nu}$ and $\beta = \frac{1-\gamma}{2(1-2\gamma)}$.

The stress-energy tensor for anisotropic matter is given by:

$$T_{\mu\nu} = (\epsilon + p_t) U_\mu U_\nu + p_t g_{\mu\nu} - \sigma k_\mu k_\nu. \tag{9}$$

U_μ and k_μ are unit four-vectors that must satisfy $U_\mu U^\mu = -1$, $k_\mu k^\mu = 1$, and $U_\mu k^\mu = 0$. We can see that when $\sigma = 0$, the fluid becomes isotropic, denoting a fluid with equal pressure in all directions.

In anisotropic matter, the trace of the stress - energy tensor is:

$$T = 3p_r + 2\sigma - \epsilon. \tag{10}$$

We then obtain the modified TOV equations for the anisotropic star structure in Rastall's gravity:

$$\frac{dm}{dr} = 4\pi r^2 \epsilon^{\text{eff}}, \tag{11}$$

$$\frac{dp_r}{dr} = \left[-\frac{(p_r{}^{\text{eff}} + \epsilon^{\text{eff}})(m + 4\pi r^3 p_r{}^{\text{eff}})}{r(r-2m)} + \frac{2\sigma}{r} \right] \times \frac{1}{\left[1 - 3\beta - 2\beta \frac{d\sigma}{dp_r} + \beta \frac{d\epsilon}{dp_r} \right]}, \tag{12}$$

$$\frac{d\nu}{dr} = \frac{1}{2r} \left[(1 - 8\pi p_r{}^{\text{eff}} r^2) e^{2\lambda} - 1 \right] \tag{13}$$

where the effective matter variables $p_r{}^{\text{eff}}$ and ϵ^{eff} have the values:

$$p_r{}^{\text{eff}} = p_r - \beta T,$$
$$\epsilon^{\text{eff}} = \epsilon + \beta T.$$

The TOV equations above can be solved by applying the boundary conditions at the star's center ($r = 0$) and the star's surface($r = R$):

$$p_r(0) = p_{r(c)} \quad , \qquad p_r(R) = 0 \tag{14}$$

$$m(0) = 0 \quad , \qquad m(R) = M \tag{15}$$

$$\nu(0) = \nu_c \quad , \qquad \nu(R) = \frac{1}{2} \ln \left[1 - \frac{2M}{R} \right]. \tag{16}$$

By supplying an equation of state for energy density as a function of pressure, and taking into account anisotropy factors as a metric, numerical solutions are obtained computationally using iterative schemes, such as the fourth-order Runge-Kutta method. In this work, we study the allowed values of β based on the stability conditions for compact objects.

5 Tidal deformability

Compact stars inevitably experience geometric deformations due to tidal forces induced by nearby massive bodies. These deformations are quantified by the tidal deformability parameter λ, which relates the induced quadrupole moment Q_{ij} to the external tidal field [Oeveren, 2018]:

$$Q_{ij} = -\lambda \varepsilon_{ij}. \tag{17}$$

Q_{ij} is the induced quadrupole moment tensor, and ε_{ij} is the tidal field tensor.

The parameter λ is further linked to the dimensionless ($l = 2$) quadrupolar tidal Love number k_2 and the stellar radius R:

$$\lambda = \frac{2}{3} k_2 R^5. \tag{18}$$

A dimensionless tidal deformability, $\Lambda = \frac{\lambda}{M^5} = \frac{2}{3} \frac{k_2}{C^5}$, can also be defined, where $C = \frac{M}{R}$ is the compactness of the star.

We can write the spacetime metric $g_{\mu\nu}$ of a fluid under tidal perturbations as:

$$g_{\mu\nu} = g^0_{\mu\nu} + h_{\mu\nu}, \tag{19}$$

where $g^0_{\mu\nu}$ is a static unperturbed metric such as the spherically symmetric metric in Eq. (7), and $h_{\mu\nu}$ is the linearized metric perturbation caused by tidal effects [Thorne and Campolattaro, 1967].

In this research, we will be analyzing only the static, even-parity perturbations in the Regge-Wheeler gauge [Regge and Wheeler, 1957]. The tidal perturbation metric is given by [Hinderer, 2008]:

$$h_{\mu\nu} = \mathrm{diag}[-e^{\nu} H_0, e^{\lambda} H_2, r^2 K, r^2 \sin^2 \theta K] Y_{2m}. \tag{20}$$

H_0, H_2, and K are functions of r, while Y_{2m} is a function of (θ, ϕ). Substituting this expression into the linearized Einstein field equations and using

an anisotropic fluid model yields a system where only diagonal components of the perturbed stress-energy tensor are nonzero. This leads to the following relations:

$$H_0 = -H_2 \equiv H, \tag{21}$$

$$K' = 2H\nu' + H', \tag{22}$$

$$\delta p_t = \frac{H}{8\pi r} e^{-2\lambda}(\lambda' + \nu') Y_{2m}. \tag{23}$$

Combining components of the perturbed Einstein tensor yields a second-order differential equation for $H(r)$. [Biswas and Bose, 2019]:

$$H'' + PH' + QH = 0, \tag{24}$$

where, for GR theory,

$$P \equiv \frac{2}{r} + e^{2\lambda}\left[\frac{2m}{r^2} + 4\pi r(p_r - \epsilon)\right], \tag{25}$$

$$Q \equiv 4\pi e^{2\lambda}\left[4\epsilon + 8p_r + \frac{\epsilon + p_r}{Av_s^2}(1 + v_s^2)\right] - \frac{6e^{2\lambda}}{r^2} - 4\nu'^2, \tag{26}$$

with the values $A \equiv \frac{dp_t}{dp_r}$ and the radial speed of sound $v_s^2 \equiv \frac{dp_r}{d\epsilon}$. We can rewrite Eq. (24) as a first-order differential equation of the internal structure:

$$ry' + y^2 + yF + r^2 Q = 0, \tag{27}$$

where

$$y(r) \equiv = y_{\text{internal}}(r) = r\frac{H'}{H}, \tag{28}$$

$$F(r) \equiv rP - 1. \tag{29}$$

Eq. (27) can be solved together with the TOV equations with the boundary condition in center, $y(0) = l = 2$. We use the value $l = 2$ because it is the quadrupole mode that primarily contributes to the tidal deformation of compact stars (deforming the star into oblate or prolate shapes under the influence of an external tidal field). Higher multipoles ($l \geq 3$) have much less significant effect on the overall physical effect of tidal deformations, and therefore are negligible in the case of our research. It is worth noting that in cases like higher precision measurements and specific multipole studies, different modes of l may be considered. At the solar exterior, we can rewrite Eq. (24) with a form associated with the Legendre equation with $l = m = 2$ by defining $x \equiv \frac{r}{m} - 1$ [Thorne and Campolattaro, 1967]. Then we can write H as the Legendre functions P_2^2 and Q_2^2:

$$(x^2 - 1)H'' + 2xH' - 6(6 + \frac{4}{x^2 - 1})H = 0, \tag{30}$$

$$H = a_P P_2^2(x) + a_Q Q_2^2(x). \tag{31}$$

where a_P and a_Q are coefficients to be determined. The external structure can be written as a function of the previously defined x:

$$y_{\text{external}}(x) \equiv r\frac{H'}{H} = (1+x)\frac{(P_2^2)'(x) + a(Q_2^2)'(x)}{P_2^2(x) + aQ_2^2(x)}, \tag{32}$$

where $a \equiv \frac{a_Q}{a_P}$.

Matching the internal and external solutions of H at the surface of the star ($r = R$) leads us to the solution for the Love number k_2 [Damour and Nagar, 2009]:

$$\begin{aligned} k_2 = \frac{8}{5}(1-2C)^2C^5[2C(y_R-1)-y_R+2]\,\big[2C[4(y_R+1)C^4 \\ +(6y_R-4)C^3 + (26-22y_R)C^2 + 3(5y_R-8)C - 3y_R \\ +6] + 3(1-2C)^2[2C(y_R-1)-y_R+2]\log(1-2C)\big]^{-1}. \end{aligned} \tag{33}$$

Notably, in both General Relativity and Rastall gravity, the expression for k_2 remains formally the same in vacuum [Meng and Liu, 2021]. However, the calculation of y_R must account for the modified gravitational dynamics under the Rastall framework by adjusting the P and Q terms. This can be obtained by simply replacing pressure and energy densities with their effective counterparts:

$$P \equiv \frac{2}{r} + e^{2\lambda}\left[\frac{2m}{r^2} + 4\pi r(p_r^{\text{eff}} - \epsilon^{\text{eff}})\right], \tag{34}$$

$$Q \equiv 4\pi e^{2\lambda}\left[4\epsilon^{\text{eff}} + 8p_r^{\text{eff}} + \frac{\epsilon + p_r}{Av_s^{2\,\text{eff}}}(1+v_s^2)\right] - \frac{6e^{2\lambda}}{r^2} - 4\nu'^2, \tag{35}$$

where we apply similar modifications to the radial speed of sound $v_s^{2\,\text{eff}} \equiv \frac{dp_r^{\text{eff}}}{d\epsilon^{\text{eff}}}$.

6 Moment of inertia

In GR, rotating relativistic fluids drag nearby inertial frames. This is a phenomenon known as frame dragging. To analyze slowly rotating compact stars, a small rotational correction is added to the static spacetime metric. This correction introduces an off-diagonal component involving the angular velocity function $\omega(r,\theta)$, and the resulting metric is based on the Hartle – Thorne formalism.

$$ds^2 = ds_0^2 + ds_{\text{SR}}^2, \tag{36}$$

$$ds_{\text{SR}}^2 = -2\omega(r,\theta)r^2\sin^2\theta dt d\phi. \tag{37}$$

A key quantity is the relative angular velocity $\bar{\omega} = \Omega - \omega$, where Ω is the star's rotational (Keplerian) angular velocity and ω is the angular velocity measured by a freely falling observer.

The first-order field equation gives:

$$\frac{1}{r^4}\frac{\partial}{\partial r}\left(r^4 j \frac{\partial \bar{\omega}}{\partial r}\right) + \frac{4}{r}\frac{dj}{dr}\bar{\omega} + \frac{e^{(\lambda-\nu)/2}}{r^2}\frac{1}{\sin^3\theta}\frac{\partial}{\partial\theta}\left(\sin^3\theta\frac{\partial\bar{\omega}}{\partial\theta}\right) = 0, \tag{38}$$

where $j = j(r) = e^{-(\lambda+\nu)/2}$ [Hartle, 1967].

However, if we include anisotropic pressure, $\bar{\omega}$ can be redefined with Legendre polynomials P_l [Regge and Wheeler, 1957]:

$$\bar{\omega}(r,\theta) = \sum_{l=1}^{\infty}\bar{\omega}_l(r)\left(-\frac{1}{\sin\theta}\frac{dP_l}{d\theta}\right). \tag{39}$$

Expansion of the polynomials shows that all the coefficients of $\bar{\omega}$ vanish except for the case $l = 1$. The differential equation (38) becomes:

$$\frac{1}{r^4}\frac{d}{dr}\left(r^4 j\frac{d\bar{\omega}}{dr}\right) + \frac{4}{r}\frac{dj}{dr}\bar{\omega} = 0. \tag{40}$$

If we include anisotropic pressure, Eq. (40) becomes [L. Peterson, 2021]:

$$\frac{1}{r^4}\frac{d}{dr}\left(r^4 j\frac{d\bar{\omega}}{dr}\right) + \frac{4}{r}\frac{dj}{dr}(1+\frac{\sigma}{\epsilon+p_r})\bar{\omega} = 0. \tag{41}$$

Recalling that in Rastall gravity, we keep the standard form of the gravitational equations and introduce Rastall effects through the modified matter sector, we can use the GR-based Eq. (41) to compute the inertial properties of the compact star. These are later combined with the Rastall effects through the background metric and matter profiles obtained from the modified TOV equations.

To obtain the moment of inertia, we define $\tilde{\omega}$=$\bar{\omega}/\Omega$ and rewrite Eq. (41) as two coupled first-order differential equations $\frac{d\tilde{\omega}}{dr}$ and $\frac{d\tilde{\kappa}}{dr}$. These expressions serve as auxiliary functions that allow for a simpler mathematical computation [Rahmansyah et al., 2020]:

$$\begin{aligned}\frac{d\tilde{\omega}}{dr} &= \frac{6}{r^4}e^{\nu}\left(1-\frac{2m}{r}\right)^{-1/2}\tilde{\kappa},\\ \frac{d\tilde{\kappa}}{dr} &= \frac{8\pi}{3}\frac{r^4 e^{-\nu}(\epsilon+p_r)}{(1-\frac{2m}{r})^{1/2}}\left(1-\frac{\sigma}{\epsilon+p_r}\right)\tilde{\omega}.\end{aligned} \tag{42}$$

We solve the two first-order differential equations using the Runge–Kutta methods with boundary conditions:

$$\begin{aligned}\tilde{\omega}(R) &= 1-\frac{2I}{R^3},\\ \tilde{\kappa}(R) &= I,\end{aligned} \tag{43}$$

where, I is the moment of inertia of the compact star.

7 Energy conditions

In the framework of general relativity, the constraints and energy condition rules to ensure a physically acceptable star are as follows:

1. The energy-momentum tensor must obey the dominant and strong energy conditions (DEC and SEC);
2. The energy density and pressures must remain positive inside the star, monotonically decreasing toward the surface;
3. The speeds of sound must be positive and always slower than the speed of light inside the star;
4. At the surface of the star, the radial pressure must vanish. Additionally, both the radial and tangential pressures must be equal at the center of the stellar matter configuration.

7.1 DEC and SEC with different anisotropy values

The dominant and strong ECs are defined by:

- DEC: $\epsilon - p_r - 2p_t > 0$
- SEC: $\epsilon + p_r + 2p_t > 0$

Fig. 1 shows the effect of varying anisotropy values, both positive and negative, on the dominant energy condition (DEC) and strong energy condition (SEC) evaluated at the stellar surface for configurations with different central pressures. The results indicate that the energy conditions remain valid for small anisotropy values, specifically within the range $\alpha = \pm 0.0001$. However, when the magnitude of anisotropy increases beyond this range, the structure of the star starts to fall outside the physically acceptable numerical bounds. Large positive anisotropy values lead to the violation of the DEC (as shown in the leftmost panel), while large negative anisotropy values lead to the violation of the SEC (as shown in the rightmost panel). The ECs are evaluated at the center of the star ($r = 0$), where the configuration is most compact. If the ECs are satisfed at the center, they will also be satisfied as they approach the surface ($0 \leq r \leq R$). This trend is illustrated in Fig. 2. Fig. 2 demonstrates that both the dominant and strong energy conditions are satisfied for all considered anisotropic parameters in the range $-0.0001 \leq \alpha \leq 0.0001$. In these plots, the energy conditions are evaluated throughout the stellar interior, from the center to the surface ($0 \leq r \leq R$), for configurations at the expected maximum mass limit. This confirms the physical viability of Chaplygin dark stars within these bounds. The analysis was further extended to the Rastall gravity framework, with parameter values $-0.05 \leq \beta \leq 0.05$. It was again verified that the adopted model remains consistent. The simultaneous fulfillment of both energy conditions across these ranges reinforces the robustness of the theoretical framework. This indicates that neither the introduction of small anisotropy values nor the modifications arising from Rastall gravity result in extreme behaviors in the matter distribution. These results demonstrate that the proposed stellar model satisfies the fundamental requirements of a realistic compact object and can be regarded as consistent in both classical GR and its Rastall extension.

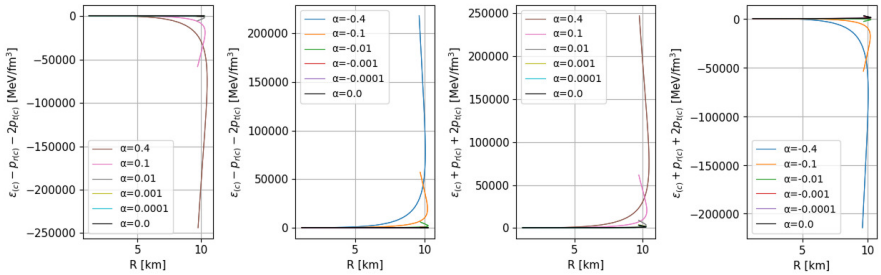

Fig. 1. ECs for anisotropic dark stars at various star radii, calculated at the center. (From the left) First panel: DEC for positive anisotropy values (out of bounds). Second panel: DEC for negative anisotropy values. Third panel: SEC for positive anisotropy values. Fourth panel: SEC for negative anisotropy values (out of bounds).

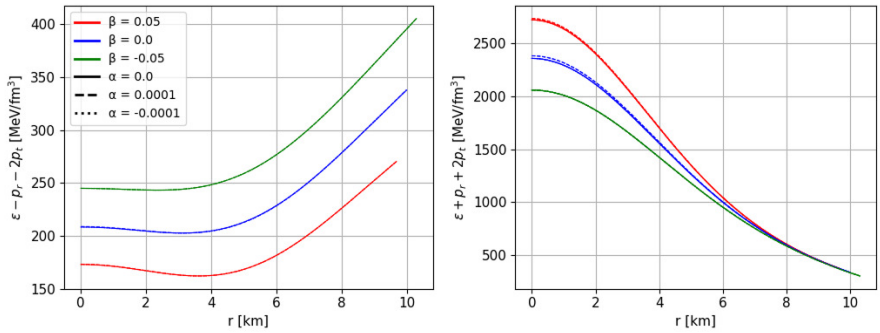

Fig. 2. ECs in physically possible anisotropic dark stars in Rastall's gravity for $0 \leq r \leq R$ (computed for the star at the expected maximum mass configuration). Left panel: DEC. Right panel: SEC, both as a function of star radius R.

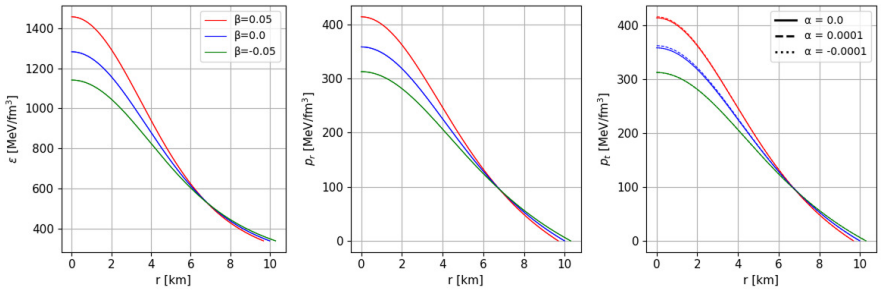

Fig. 3. Internal star profile for $0 \leq r \leq R$ (computed for the star at the expected maximum mass configuration). Left panel: energy density. Middle panel: radial pressure. Right panel: tangential pressure (with anisotropy present).

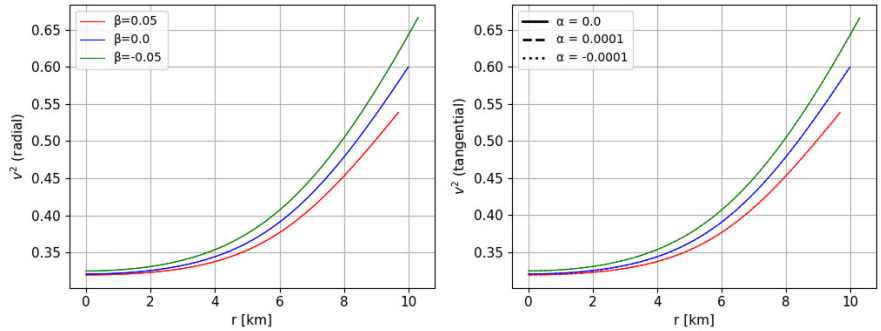

Fig. 4. Internal speeds of sound for $0 \leq r \leq R$ (computed for the star at the expected maximum mass configuration). Left panel: radial speed of sound. Right panel: tangential speed of sound (with anisotropy present)

7.2 Physical viability in Rastall gravity

Figs. 3 and 4 illustrate how the star's physical viability satisfies the second and third energy conditions under Rastall gravity. In Fig. 3, the internal stellar profiles for $0 \leq r \leq R$, computed for the star at the expected maximum mass configuration are shown. The left, middle, and right panels correspond to the energy density, radial pressure, and tangential pressure. All quantities decrease monotonically with increasing radius. This is consistent with what is expected for a physically realistic compact object. As in earlier plots, the presence of anisotropy produces only minor deviations that do not significantly affect the overall trends of the matter distribution.

Fig. 4 shows the internal radial (left panel) and tangential (right panel) speeds of sound for $0 \leq r \leq R$ (computed for the star at the expected maximum mass configuration). For stars with smaller masses of M, central densities and central pressures decrease, resulting in smaller speeds of sound that eventually approach zero. These plots show that both radial and tangential speeds of sound are subluminal ($v^2 < 1$). The interior matter of the star remains stable avoiding cracking or overturning. If a larger anisotropic magnitude were applied, the interior stellar structure might experience a reversal of forces. In this case, attractive forces could become repulsive at certain points inside the star [Chan et al., 1993].

At the end of this section, we identify the ranges of the parameters α and β that align with the energy conditions for the adopted equation of state: $-0.0001 \leq \alpha \leq 0.0001$ and $-0.05 \leq \beta \leq 0.05$. These parameters directly affect the physical properties of the stellar configurations. Our analysis indicates that the Rastall parameter β plays a more significant role than the anisotropy parameter α. It should be noted that the present configurations are valid only for our chosen parameter set. Physical viability is not guaranteed for other parameter choices. Drastic changes to the equation of state will likely impact the physical viability and the mass–radius relation of the star.

8 Results and Discussions

8.1 Stellar Structure

The plots in both panels of Fig. 5 show that the Rastall parameter β significantly affects the EoS and the stellar structure. A positive β ($\beta = 0.05$) reduces the maximum mass of the star, while a negative β ($\beta = -0.05$) increases it. A negative β makes the star less tightly bound, allowing for higher-mass stability. Conversely, a positive β restricts the formation of massive compact stars. This behavior stems from the non-conservation of matter in Rastall's stress-energy tensor. The left panel also shows anisotropic configurations, but the lines are barely discernible because their differences from the isotropic cases are negligible.

The compactness $C \equiv M/R$ is shown in the right panel of Fig. 5. The results are consistent with the mass–radius relation: a negative β allows for a higher mass at a given radius, while a positive β lowers this threshold. Thus, Rastall gravity directly influences both the maximum mass and the compactness of viable stars.

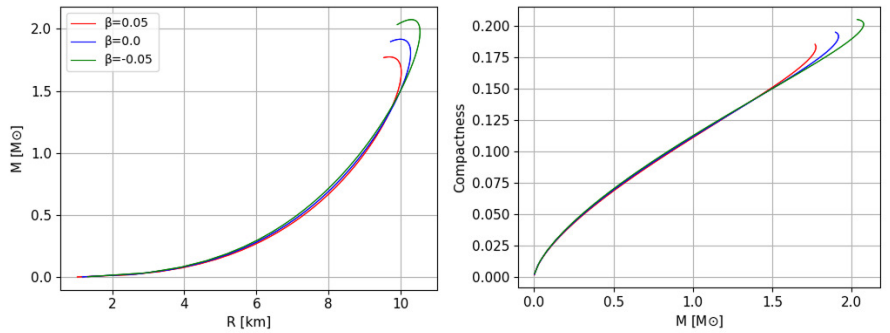

Fig. 5. Left panel: mass-radius configurations. Right panel: compactness as a function of M.

Although the anisotropy factor does not produce a significant change in the mass-radius relation, it plays a key role in shaping the tangential pressure of the star, where the tangential pressure refers to the force exerted perpendicular to the radial direction within the stellar material. To illustrate this, Fig. 6 shows the radial (directed toward the center of the star) and tangential pressures as functions of the stellar radius. In particular, the influence of anisotropy—defined as the difference between the radial and tangential pressures—is more evident in the tangential pressure plots, consistent with the definition $\sigma = p_t - p_r$. Moreover, the impact of the effective pressures, p_r^{eff} (effective radial pressure) and p_t^{eff} (effective tangential pressure), becomes clear under different values of the Rastall parameter.

The left panel of Fig. 7 displays the relation between the stellar mass M and the central energy density ϵ_c. In the Rastall framework, stars with identical central densities ϵ_c reach higher masses M for negative β values

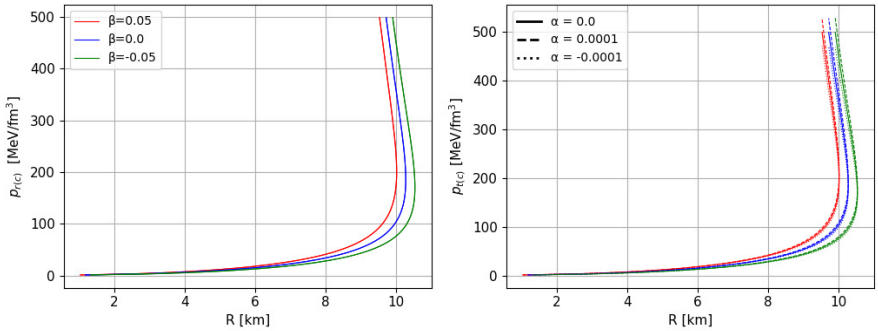

Fig. 6. Left panel: radial pressure. Right panel: tangential pressure (with anisotropy present), both as a function of R.

and lower masses for positive β values, compared to GR. The overall trend remains close to the GR curve, since the nonconserved stress-energy tensor $T_{\mu\nu}$ depends only on the pressure p and energy density ϵ. This reflects the effect of the nonminimal matter-geometry coupling, which modifies the maximum mass that can be achieved at a given central density. The right panel of Fig. 7 shows the gravitational redshift z_{sur} as a function of the central energy density ϵ_c, defined by the following equation:

$$z_{sur} = e^{\lambda} - 1 = \left(1 - \frac{2m}{r}\right)^{-\frac{1}{2}} - 1. \tag{44}$$

The gravitational redshift describes the strength of the curvature of spacetime at the surface of the star. This redshift reflects the star's compactness: for low-mass (less compact) stars, the effect is negligible, while in more massive (more compact) stars, the effect becomes pronounced. Specifically, the maximum redshift increases for negative Rastall parameters and decreases for positive ones. A higher redshift corresponds to stronger spacetime curvature, making the star more relativistic. However, the maximum values remain well below the extreme limit $z_{\rm sur} \to 1$, indicating that dark stars in Rastall modified gravity remain physically stable.

Table 1 presents the stellar radius and mass configurations at central pressure $p_r = 101$ MeV/fm^3, along with the corresponding energy density and gravitational redshift values. Only the presence of a nonzero Rastall parameter alters the energy density; anisotropy parameters induce negligible changes in all stellar properties. As the Rastall parameter β increases, the central mass, radius, energy density, and gravitational redshift decrease. A positive Rastall parameter represents a stronger coupling between geometry and matter inside the star, implying that energy-momentum is not conserved and the energy density predicted by Rastall gravity can either increase or decrease, depending on the specific value of the parameter.

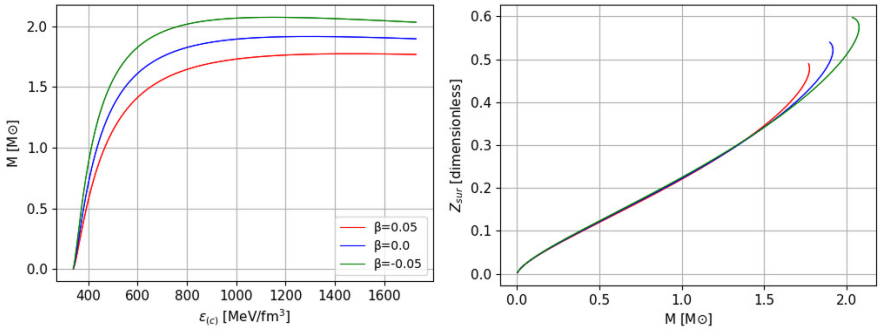

Fig. 7. Left panel: Energy density vs M. Right panel: Gravitational redshift vs M.

Table 1. Configurations for $p_r = 101$ MeV/fm^3 with different Rastall parameters and anisotropic perturbations

β	α	Mass [$M_\odot$]	Radius [km]	ϵ [MeV/fm^3]	z_{sur} [dimensionless]
-0.05	-0.0001	1.708822	10.312401	558.382887	0.400951
	0	1.708873	10.312501	557.88815	0.400965
	+0.0001	1.708924	10.312601	557.393394	0.400978
0	-0.0001	1.489227	9.970901	545.750619	0.338816
	0	1.489235	9.970901	545.750619	0.338819
	+0.0001	1.48928	9.971001	545.750619	0.33883
+0.05	-0.0001	1.289474	9.623101	533.213019	0.287388
	0	1.289481	9.623101	533.613088	0.28739
	+0.0001	1.289521	9.623201	534.013167	0.287399

8.2 Tidal properties

The leftmost panel of Fig. 8 depicts the dimensionless, electric-type tidal Love number k_2 (which quantifies how readily a star deforms in response to a tidal field) as a function of the dark star's compactness, defined as the ratio of the star's mass to its radius. The results show that larger values of the Rastall parameter correspond to higher maximum k_2 values for the Chaplygin dark star. This demonstrates that Rastall modified gravity directly affects the star's susceptibility to deformation under an external tidal field.

We also examine the tidal parameter λ (middle panel), which characterizes the star's deformability under an external gravitational field, and the corresponding dimensionless tidal deformability Λ (rightmost panel), defined as a scaled measure of λ relative to the star's compactness. The numerical values of Λ at the maximum stellar mass are provided in Table 2. As with the Love number results, the tidal effects increase or decrease depending on the chosen Rastall parameter β. For the Chaplygin dark star equation of state used here, no qualitative changes are observed in the overall trends of the tidal deformability.

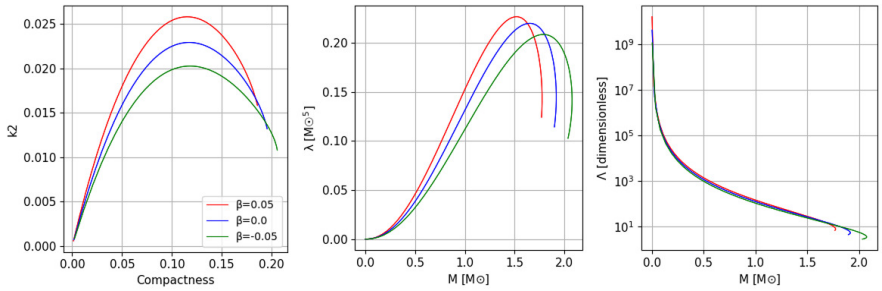

Fig. 8. Left panel: Electric tidal Love number as a function of compactness. Middle panel: Tidal parameter as a function of M. Right panel: Dimensionless tidal deformability as a function of M.

Table 2. Dimensionless tidal deformability Λ at $M = M_{\max}$ with different Rastall parameters

β	$M_{\max}$ [M$\odot$]	Λ at $M_{\max}$ [dimensionless]
-0.05	2.075173	3.477274
0	1.916892	5.30122
+0.05	1.774664	7.667622

The obtained tidal deformability arises from quadrupolar perturbations to the equilibrium configuration. In Rastall's framework, this tidal effect is significantly amplified or suppressed in the high-mass region; by contrast, the differences remain negligible in the low-mass region. As expected, increasing compactness leads to a decrease in tidal deformability, indicating that more compact stars are less deformable. Moreover, these results suggest that the Rastall parameter has little to no impact on stars with low compactness. Finally, for the Chaplygin dark star model, configurations with very small stellar masses exhibit extremely high tidal deformability.

8.3 Rotational properties

We calculate the moment of inertia of the Chaplygin dark star by incorporating the slow-rotation sector into our metric. As shown in the left panel of Fig. 9, the moment of inertia decreases as the Rastall parameter β increases, especially for high stellar masses. This inverse relationship implies that higher values of β allow stars to attain faster rotation rates. The right panel of Fig. 9 further illustrates these findings by showing how the dimensionless moment of inertia varies with stellar compactness.

These plots visualize effects of the slow-rotating perturbations on our dark star model. The moment of inertia naturally increases with mass. However, beyond a certain point, the moment of inertia reaches a maximum and then decreases, indicating the existence of a maximum allowable moment of inertia.

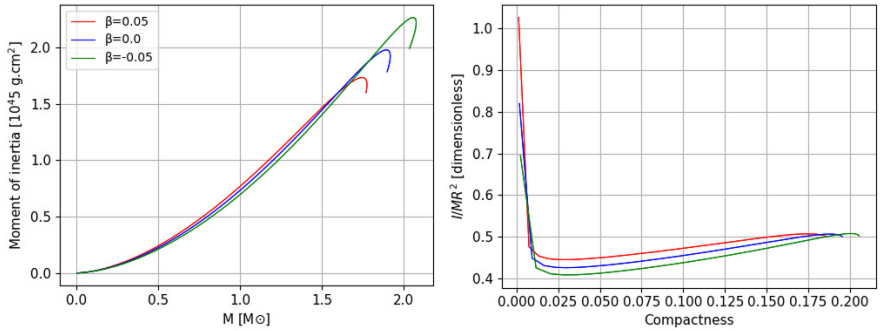

Fig. 9. Left panel: Moment of inertia. Right panel: Dimensionless moment of inertia, both for certain β variations for a fixed α value.

We define the relative difference ΔI of the moment of inertia to better quantify the effects of Rastall gravity and anisotropyf:

$$\Delta I = \frac{I_{i\max} - I_{0\max}}{I_{i\max}}, \tag{45}$$

$I_{0\max}$ is the maximum moment of inertia for isotropic stars in GR ($\beta = 0$), and $I_{i\max}$ is the corresponding quantity for stars with Rastall effects. Table 3 shows the ΔI values. The Rastall parameter β decreases ΔI almost linearly; larger β values correspond to smaller differences in moment of inertia. This trend is consistent with changes in other stellar properties observed within the Rastall framework.

Table 3. Maximum moment of inertia $I_i$max and the relative difference ΔI with different Rastall and anisotropy values

β	$I_i$max [10^{45} g.cm^2]	ΔI [%]
-0.05	2.264757	14.493
0	1.978083	0 (default)
+0.05	1.732429	-12.419

To conclude this section, our research highlights the role of Rastall gravity—a modified gravitational theory that alters standard conservation laws—in changing key stellar properties. The analysis reveals significant effects on the mass–radius relation, compactness, pressure distribution, energy density, and redshift, with systematic shifts in the predicted maximum stellar masses for different Rastall scenarios. These changes also affect observable quantities, such as the tidal deformability and the moment of inertia. We found that

adding a miniscule anisotropic effect to the Chaplygin dark star produces only minor changes in the overall stellar behavior, largely independent of the values of the Rastall parameter values. Overall, these findings suggest that departures from GR can leave measurable marks on the structure and dynamics of dark stars.

9 Conclusions

This study examined the structure of anisotropic dark stars described by the generalized Chaplygin equation of state within the framework of Rastall gravity. The modified Tolman–Oppenheimer–Volkoff equations were derived and solved for various values of the Rastall parameter β and the anisotropy parameter α. Tests of the DEC and SEC were incorporated to identify the physically viable parameter ranges.

From the energy-condition tests, we found that, for Chaplygin EoS parameters A = 0.3 and B = $6.010^{-20}m^{-4}$, the resulting dark star solutions remain physically acceptable only for $-0.0001 \leq \alpha \leq 0.0001$ and $-0.05 \leq \beta \leq 0.05$. The Rastall parameter β has a stronger influence on the star's structure than the anisotropy parameter α. This influence extends from the basic mass-radius relations to tidal deformability and moment of inertia configurations. Our analysis showed that increasing β leads to less compact dark stars, while negative β values enable the construction of stars with larger maximum masses. These results are valid for our chosen Chaplygin EoS parameter set; therefore, physical viability cannot be guaranteed for other parameter choices. Nevertheless, we expect our conclusions to remain generally applicable to Chaplygin equations of state that satisfy the ECs.

We conclude that departures from General Relativity, such as Rastall gravity, may produce observable effects on the structure and dynamics of dark stars.

References

Abbas, G. and Shahzad, M. (2019). Models of anisotropic compact stars in the rastall theory of gravity. *Astrophysics and Space Science*, 364:50.

Abbas, G. and Shahzad, M. R. (2018). A new model of quintessence compact stars in the rastall theory of gravity. *The European Physical Journal A*, 54(12).

Abbott, R. et al. (2020). Gw190814: Gravitational waves from the coalescence of a 23 solar mass black hole with a 2.6 solar mass compact object. *The Astrophysical Journal Letters*, 896(2):L44.

Antoniadis, J., Freire, P. C. C., Wex, N., Tauris, T. M., Lynch, R. S., van Kerkwijk, M. H., Kramer, M., Bassa, C., Dhillon, V. S., Driebe, T., Hessels, J. W. T., Kaspi, V. M., Kondratiev, V. I., Langer, N., Marsh, T. R., McLaughlin, M. A., Pennucci, T. T., Ransom, S. M., Stairs, I. H., van Leeuwen, J., Verbiest, J. P. W., and Whelan, D. G. (2013). A massive pulsar in a compact relativistic binary. *Science*, 340(6131).

Banerjee, A., Pradhan, A., Sakalli, I., and Dixit, A. (2024). Properties of interacting quark star in light of rastall gravity.

Benaoum, H. (2002). Accelerated universe from modified chaplygin gas and tachyonic fluid. *Universe*, 8(7).

Bento, M. C., Bertolami, O., and Sen, A. (2002). Generalized chaplygin gas, accelerated expansion and dark energy-matter unification. *Phys. Rev. D*, 66.

Bhar, P. (2021). Dark energy stars in tolman–kuchowicz spacetime in the context of einstein gravity. *Physics of the Dark Universe*, 34:100879.

Bhar, P., Govender, M., and Sharma, R. (2018). Anisotropic stars obeying chaplygin equation of state. *Pramana - J Phys*, 90(5).

Biswas, B. and Bose, S. (2019). Tidal deformability of an anisotropic compact star: Implications of gw170817. *Phys. Rev. D*, 99.

Biswas, S., Bhattacharjee, D., and Chattopadhyay, P. K. (2025). Maximum mass of singularity-free anisotropic compact stars in rastall theory of gravity.

Bowers, R. L. and Liang, E. P. T. (1974). Anisotropic spheres in general relativity. *Astrophysical Journal*, 188:657.

Cadoni, M., Sanna, A. P., and Tuveri, M. (2020). Anisotropic fluid cosmology: an alternative to dark matter? *Phys. Rev. D*, 102:023514.

Calogero, S. and Velten, H. (2013). Cosmology with matter diffusion. *Journal of Cosmology and Astroparticle Physics*, 2013(11):025.

Chadha-Day, F., Ellis, J., and Marsh, D. J. E. (2022). Axion dark matter: What is it and why now? *Science Advances*, 8.

Chagoya, J., López-Domínguez, J. C., and Ortiz, C. (2023). Cosmological fluids in the equivalence between rastall and einstein gravity. *Classical and Quantum Gravity*, 40(7):075005.

Chan, R., Herrera, L., and Santos, N. O. (1993). Dynamical instability for radiating anisotropic collapse. *Monthly Notices of the Royal Astronomical Society*, 265.

Damour, T. and Nagar, A. (2009). Relativistic tidal properties of neutron stars. *Phys. Rev. D*, 80.

Darabi, F., Moradpour, H., Licata, I., Heydarzade, Y., and Corda, C. (2018). Einstein and rastall theories of gravitation in comparison. *The European Physical Journal C*, 78(1).

Demorest, P. B., Pennucci, T., Ransom, S. M., Roberts, M. S. E., and Hessels, J. W. T. (2010). A two-solar-mass neutron star measured using shapiro delay. *Nature*, 467(7319):1081–1083.

dos Santos, R. V. and Nogales, J. A. C. (2017). Cosmology from a lagrangian formulation for rastall's theory.

Estevez-Delgado, J., Duran, M. P., Cleary-Balderas, A., Maya, N. E. R., and Peña, J. M. (2021). Chaplygin strange stars in presence of quintessence. *Modern Physics Letters A*, 36(29).

Fabris, J., Piattella, O., and Rodrigues, D. (2023). On rastall gravity formulation as a f(r,lm) and a f(r, t) theory. *The European Physical Journal Plus*, 138:232.

Fisher, S. B. and Carlson, E. D. (2019). Reexamining $f(r, t)$ gravity. *Physical Review D*, 100(6).

Gelmini, G. B. (2017). Light weakly interacting massive particles. *Rept. Prog. Phys.*, 80(8).

Glendenning, N. K. (2007). pages 19–69. Springer New York, New York, NY.

Harko, T. and Moraes, P. H. R. S. (2020). Comment on "reexamining $f(r, t)$ gravity". *Phys. Rev. D*, 101:108501.

Hartle, J. B. (1967). Slowly rotating relativistic stars. i. equations of structure. *The Astrophysical Journal*, 150.

Hinderer, T. (2008). Tidal love numbers of neutron stars. *The Astrophysical Journal*, 677(2).

Horvat, D., Ilijić, S., and Marunović, A. (2011). Radial pulsations and stability of anisotropic stars with a quasi-local equation of state. *Class. Quantum Grav.*, 28(2).

Ilie, C., Mahmud, S. S., Paulin, J., and Freese, K. (2025). Spectroscopic supermassive dark star candidates.

Ilie, C., Paulin, J., and Freese, K. (2023). Supermassive dark star candidates seen by jwst. *Proceedings of the National Academy of Sciences*, 120(30).

Kamenshchik, A. Y., Moschella, U., and Pasquier, V. (2001). An alternative to quintessence. *Physics Letters B*, 511.

L. Peterson, A. S. (2021). Mass correction and deformation of slowly rotating anisotropic neutron stars based on hartle–thorne formalism. *Eur. Phys. J. C*, 81(698).

Meng, L. and Liu, D.-J. (2021). Tidal love numbers of neutron stars in rastall gravity. *Astrophysics and Space Science*, 366(11).

Moradpour, H., Heydarzade, Y., Darabi, F., and Salako, I. G. (2017a). A generalization to the rastall theory and cosmic eras. *The European Physical Journal C*, 77(4).

Moradpour, H., Sadeghnezhad, N., and Hendi, S. (2017b). Traversable asymptotically flat wormholes in rastall gravity. *Canadian Journal of Physics*, 95(12):1257–1266.

Moraes, W. A. G. D. and Santos, A. F. (2019). Lagrangian formalism for rastall theory of gravity and gödel-type universe.

Oeveren, E. V. (2018). *Neutron Star Tidal Deformability and Gravitational Self-force*. PhD thesis, University of Wisconsin-Milwaukee.

Oliveira, A. M., Velten, H. E. S., Fabris, J. C., and Casarini, L. (2015). Neutron stars in rastall gravity. *Phys. Rev. D*, 92.

Panotopoulos, G., Ángel Rincón, and Lopes, I. (2021). Slowly rotating dark energy stars. *Physics of the Dark Universe*, 34.

Pretel, J. M. Z. (2023). Radial pulsations, moment of inertia and tidal deformability of dark energy stars. *Eur. Phys. J. C*, 83.

Pretel, J. M. Z. and Mota, C. E. (2024). Compact stars in rastall gravity: hydrostatic equilibrium and radial pulsations. *General Relativity and Gravitation*, 56(4).

Prihadi, H. L., Sakti, M. F. A. R., Hikmawan, G., and Zen, F. P. (2020). Dynamics of charged and rotating nut black holes in rastall gravity. *International Journal of Modern Physics D*, 29(03):2050021.

Rahaman, F., Ray, S., Jafry, A. K., and Chakraborty, K. (2010). Singularity-free solutions for anisotropic charged fluids with chaplygin equation of state. *Phys. Rev. D*, 82.

Rahmansyah, A., Sulaksono, A., Wahidin, A. B., and Setiawan, A. M. (2020). Anisotropic neutron stars with hyperons: implication of the recent nuclear matter data and observations of neutron stars. *Eur. Phys. J. C*, 80(769).

Rastall, P. (1972). Generalization of the einstein theory. *Phys. Rev. D*, 6.

Regge, T. and Wheeler, J. A. (1957). Stability of a schwarzschild singularity. *Phys. Rev.*, 108.

Rizaldy, R. and Sulaksono, A. (2019). Deformation of a magnetized quark star in rastall gravity. *Journal of Physics: Conference Series*, 1321(2):022016.

Sakti, M. F., Suroso, A., and Zen, F. P. (2020). Kerr–newman–nut–kiselev black holes in rastall theory of gravity and kerr/cft correspondence. *Annals of Physics*, 413:168062.

Sakti, M. F. A. R. and Sulaksono, A. (2021). Dark energy stars with a phantom field. *Phys. Rev. D*, 103(8).

Sakti, M. F. A. R., Suroso, A., Sulaksono, A., and Zen, F. P. (2022). Rotating black holes and exotic compact objects in the kerr/cft correspondence within rastall gravity. *Physics of the Dark Universe*, 35:100974.

Shabani, H., Moradpour, H., and Ziaie, A. (2022). A dynamical system representation of generalized rastall gravity. *Physics of the Dark Universe*, 36:101047.

Smerechynskyi, S., Tsizh, M., and Novosyadlyj, B. (2021). Impact of dynamical dark energy on the neutron star equilibrium. *Journal of Cosmology and Astroparticle Physics*, 2021(02).

Tello-Ortiz, F., Malaver, M., Ángel Rincón, and Gomez-Leyton, Y. (2020). Relativistic anisotropic fluid spheres satisfying a non-linear equation of state. *Eur. Phys. J. C*, 80(371).

Thorne, K. S. and Campolattaro, A. (1967). Non-radial pulsation of general-relativistic stellar models. i. analytic analysis for l ¿= 2. *The Astrophysical Journal*, 149.

Visser, M. (2018). Rastall gravity is equivalent to einstein gravity. *Physics Letters B*, 782:83–86.

Weinberg, D. H., Mortonson, M. J., Eisenstein, D. J., Hiratae, C., Riess, A. G., and Rozo, E. (2012). Observational probes of cosmic acceleration. *Physics Reports*.

Xu, L., Lu, J., and Wang, Y. (2012). Revisiting generalized chaplygin gas as a unified dark matter and dark energy model. *The European Physical Journal C*, 72(2).

Yazadjiev, S. S. (2011). Exact dark energy star solutions. *Phys. Rev. D*, 83.